AIChE

Role of Cu on Zero Valent Bimetallic Cu—Fe in Arsenic Removal with Gas Bubbling

Piyanate Nakseedee,[a] Visanu Tanboonchuy,[b,c] Pongtanawat Khemthong,[d] Nurak Grisdanurak,[e,f] and Chih-Hsiang Liao[g]

[a]Department of Logistics Engineering, School of Engineering, University of the Thai Chamber of Commerce, Bangkok 10400, Thailand

[b]Department of Environmental Engineering, Faculty of Engineering, Khon Kaen University, 40002, Thailand

[c]Research Center for Environmental and Hazardous Substance Management (EHSM), Khon Kaen University, 40002, Thailand

[d]National Nanotechnology Center, National Science and Technology Development Agency, Pathumthani 12120, Thailand

[e]Department of Chemical Engineering, Faculty of Engineering, Thammasat University, Pathumthani 12120, Thailand

[f]Center of Excellence in Environmental Catalysis and Adsorption, Thammasat University, Pathumthani 12120, Thailand

[g]Department of Environmental Resources Management, Chia Nan University of Pharmacy and Science, Tainan 71710, Taiwan; chliao@mail.cnu.edu.tw (for correspondence)

Published online 25 March 2017 in Wiley Online Library (wileyonlinelibrary.com). DOI 10.1002/ep.12603

Arsenic (As) removal by nano bimetallic Cu-Fe synthesized by in-situ *$(Cu\text{-}Fe)_{IS}$ and impregnation $(Cu\text{-}Fe)_{IM}$ techniques was studied. Synthesized Cu-Fe by both techniques provided smaller particles than NZVI particles. $(Cu\text{-}Fe)_{IM}$ showed higher efficiency in As removal, compared to $(Cu\text{-}Fe)_{IS}$ and pristine NZVI. Batch experiments were performed by varying percent Cu loading (0–30% by wt). As(III) was removed completely by 10 wt % Cu loading on NZVI under an IM technique. It also provided double removal rate compared to pristine NZVI. X-ray absorption near edge structure analysis supported that a mixed phases of Cu_2O and CuO in $(Cu\text{-}Fe)_{IM}$ enhanced As removal toward co-precipitating with iron species about 20% for both As(III) and As(V) removal.* © 2017 American Institute of Chemical Engineers Environ Prog, 36: 1449–1457, 2017

Keywords: bimetal, XANES, gas bubbling system, Cu-NZVI

INTRODUCTION

One of major contaminants in groundwater and surface water is arsenic (As). It has been reported as a high level concentration in many countries including Bangladesh, India, China, Thailand, and Taiwan [1,2]. Its concentration was reported in a range of 10–1800 ppb, being exceed the world water quality standard for drinking water [3]. The most of predominant forms of As could be found in inorganic oxyanions of both trivalent arsenite [As(III)] and pentavalent arsenate [As(V)], where As(III) is reported to be higher toxic and difficult to remove compared with As(V) [4]. For this reason, the removal of As(III) is still one of emerging environmental investigations.

The treatment of As(III) could be enhanced by reducing the solution pH with HCl and H_2SO_4 [5,6]. However, using of such chemicals like HCl and H_2SO_4 could affect the water quality consequently. To avoid the impacts from these acidic chemicals, a treatment by employing CO_2 bubbling has been investigated [7,8]. Not only an acidic condition, but also an oxygenated condition is preferred. To increase the oxygenate environment, the gas bubbling by O_2 is directly provided. Tanboonchuy *et al.* [9] reported that a combination of two gas bubbling of CO_2 and air enhanced As(V) removal effectively, but not on As(III). The investigation revealed that the removal of As(III) required high degree of surface reactivity to ensure the suitable As(III) adsorption capacity and a sufficient contact between adsorbents-As(III). Nanoscale zero valent iron (NZVI), which contains high surface and high surface heterogeneity, has been reported as a promising adsorbent for capturing As(III)/As(V) from contaminated water [10,11].

The reactivity of NZVI has found decrease during the reaction time. This causes by the oxide layers are probably formed on NZVI particle surface. A deposition of second metal onto the NZVI surface, such as Ag, Au, Ni, Pd, and Cu, could promote the electron generation and transfer, consequently, the higher availability to reduce contaminants. The application of NZVI-based bimetals are widely used in the elimination of various pollutants such as chlorinated organic compounds, halogenated organic compounds, chromium (Cr), and lead (Pb) [12–14]. It was obvious that Pd-nanoscale iron bimetallic particles presented high efficiency in As removal. However, the application is quite limited due to extremely high cost. The alternative of Cu-nanoscale iron bimetallic particles is, therefore, desired to investigate.

Nakseedee *et al.* [15] developed successfully a NZVI coupled with CO_2-air bubbling system to enhance As removal. In this system, slightly weak acidic and dissolved oxygen assisted iron corrosion to coprecipitate As. However, As removal using Cu-NZVI coupled with CO_2-air bubbling system has not been studied. Therefore, in this context, we used Cu as a second metal on NZVI under two preparation techniques; one was an *in-situ* (IS) incorporation and the other was an impregnation (IM). The synthesized materials

were further characterized using scanning electron microscope (SEM), transmission electron microscopy (TEM). The adsorption potential for capturing of As(III)/As(V) was investigated under CO_2-air bubbling system. Influences of synthesis method and Cu loading were also reported. X-ray absorption near edge structure (XANES) technique was also used to identify expected metal species to understand the removal mechanism of As.

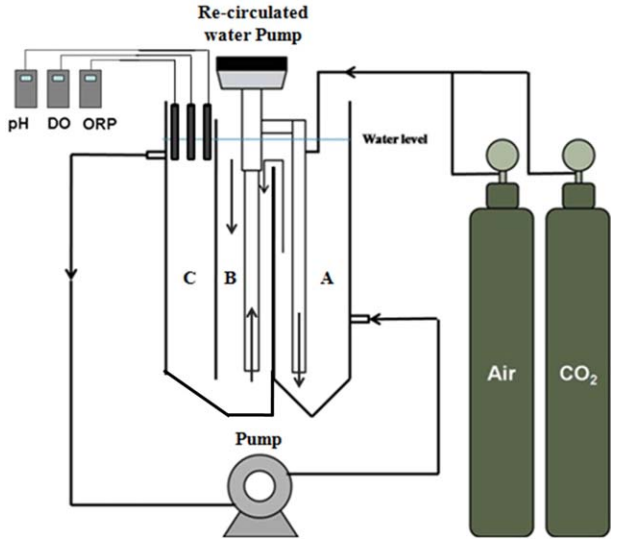

Figure 1. Experimental setup for As removal. [Color figure can be viewed at **wileyonlinelibrary.com**]

MATERIALS AND METHODS

NZVI Synthesis

The NZVI was synthesized via a reducing method, as described previously [15]; 40 mL of 0.25 M $NaBH_4$ was added into 40 mL of 0.045 M $FeCl_3$ through a pumping system (Masterflex L/S) with a feeding rate of 4 mL/min under vigorous stirring by a revolving propeller. The synthesis was carried out at room temperature. Then, NZVI was washed with DI water and applied for As removal immediately.

Syntheses of Bimetallic Nanoscale Cu—Fe Zero Valent

Bimetallic nanoscale Cu—Fe was synthesized by two techniques, under the basis of Cu mass ratio of 2.5, 5.0, 10.0, 20.0, and 30.0% (w/w).

IS Method

A mixture of $CuCl_2$ and $FeCl_3$ was prepared regarding to Cu mass ratio; 40 mL of a 0.25 M solution of $NaBH_4$ was gradually added on the prepared solution. The solution was stirred for 5 min; consequently, the obtained particles were separated from liquid solution by a magnet and being used

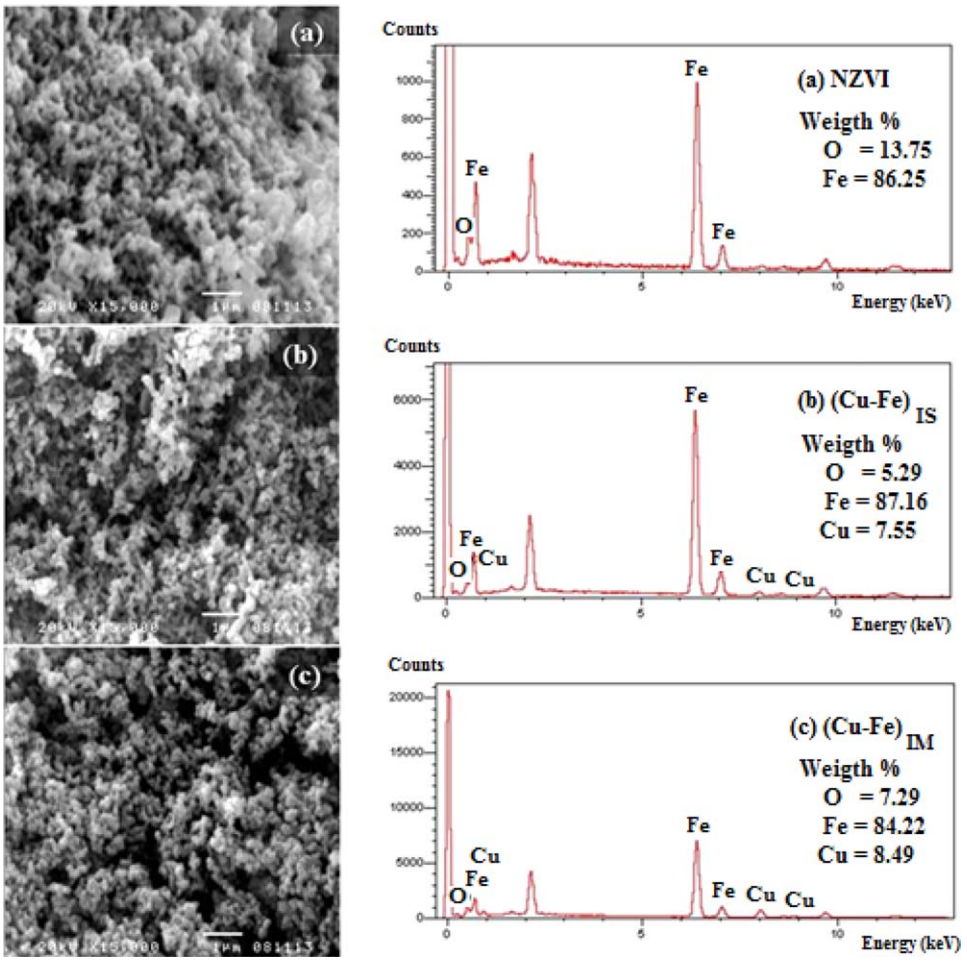

Figure 2. SEM images and the EDX profiles of: (a) NZVI, (b) $(Cu\text{-}Fe)_{IS}$, and (c) $(Cu\text{-}Fe)_{IM}$. [Color figure can be viewed at **wileyonlinelibrary.com**]

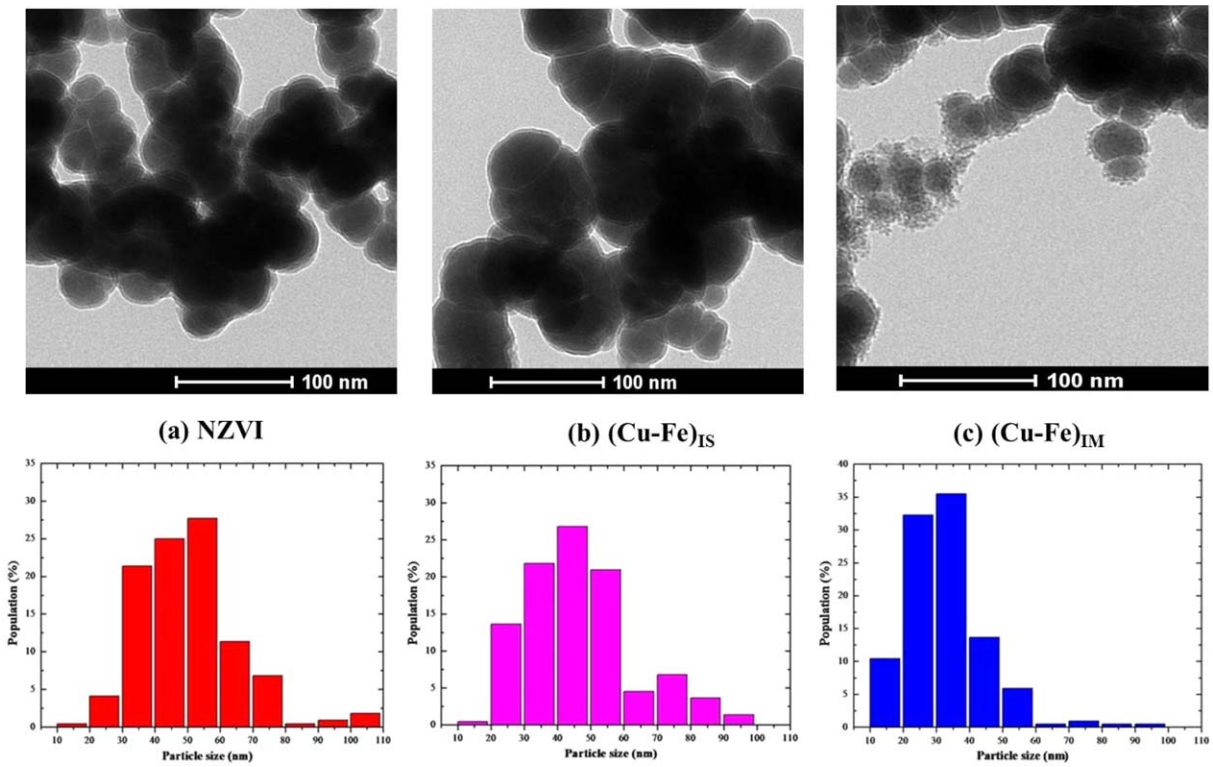

Figure 3. TEM images of: (a) NZVI, (b) $(Cu\text{-}Fe)_{IS}$, and (c) $(Cu\text{-}Fe)_{IM}$. [Color figure can be viewed at **wileyonlinelibrary.com**]

for As removal right after. Samples was denoted as $(Cu—Fe)_{IS}$. The synthesis involved a redox reaction described by the Eq. (1)

$$2Fe^{2+} + Cu^{2+} + BH^{4-} + 2H_2O \rightarrow 2Fe^0Cu^0 + BO_2^- + 4H^+ + 2H_2 \quad (1)$$

IM Method

A solution of $CuCl_2$ was prepared for 2.2 mL. The solution was added dropwise onto the pristine NZVI under the simultaneous sonication for 2 min. The obtained samples were labeled as $(Cu—Fe)_{IM}$.

As Removal Experiments

The experimental set up was displayed in Figure 1. The system with a total volume of 4.6 L was constructed with two chambers for the reaction (chambers A and B) and one chamber for particle settling (chamber C). Catalyst amount of 0.1 g was loaded into the solution, equivalent to 0.022 g/L. An initial concentration of the As-spiked groundwater was 1000 μg/L of As(III) and As(V). Before testing, the As-spiked solution was pretreated with CO_2 bubbling under the feeding rate of 300 mL/min for 5 min then switched to air bubbling with the same flow rate until the reaction was completely (∼60 min). In addition, the pH and DO values during adsorption process were continuously monitored at the top layer of reaction zone. As solution was sampled at different intervals of reaction time, and immediately filtered by a 0.45 μm membrane filter. All samples were diluted and acidified before the measurement of the total residual As concentration. Each As and total dissolved Cu and Fe were determined by ICP-OES. Replicate experiments were carried out in all batches.

Table 1. Specific surface areas of materials by BET analysis.

Materials	Surface area ($m^2\ g^{-1}$)
$(Cu—Fe)_{IS}$	22.30
$(Cu—Fe)_{IM}$	30.14
NZVI	25.63

Characterizations

Morphology of Cu-Fe samples was characterized by TEM and SEM equipped with energy dispersive X-ray (EDX). Cu and Fe K-edges of the samples were evaluated by XANES technique at BL5.2: SUT-NANOTEC-SLRI, Synchrotron Light Research Institute (Public Organization), Thailand. Data were acquired in transmission mode with an ionization chamber using helium fill gas at atmospheric pressure. The Cu and Fe K-edges was calibrated firstly with the spectra of Cu and Fe foils. All the background removal, calibration, normalization, and linear combination fitting (LCF) were processed using Athena software with standard compounds to retrieve the chemical species of the samples as described elsewhere [16]. Two sets of materials, comprised of Fe foil, FeO, Fe_3O_4, and Fe_2O_3, were chosen for Fe K-edge standards, while Cu foil, CuO, and $CuCl_2$ were selected for Cu K-edge standards.

RESULTS AND DISCUSSION

Sample Characterization

Morphologies of NZVI, $(Cu—Fe)_{IS}$, and $(Cu—Fe)_{IM}$, examined by SEM and EDX. Figure 2 shows the analysis of 10 wt % loading of Cu on NZVI, as an example. Comparing SEM images of NZVI and bimetallic Cu—Fe samples, both bimetallic $(Cu—Fe)_{IS}$ and $(Cu—Fe)_{IM}$ possessed smaller spherical particles than NZVI (confirmed in TEM analysis), indicating the Cu—Fe samples were possibly lower in aggregation property. The existence of Cu species should stabilize the

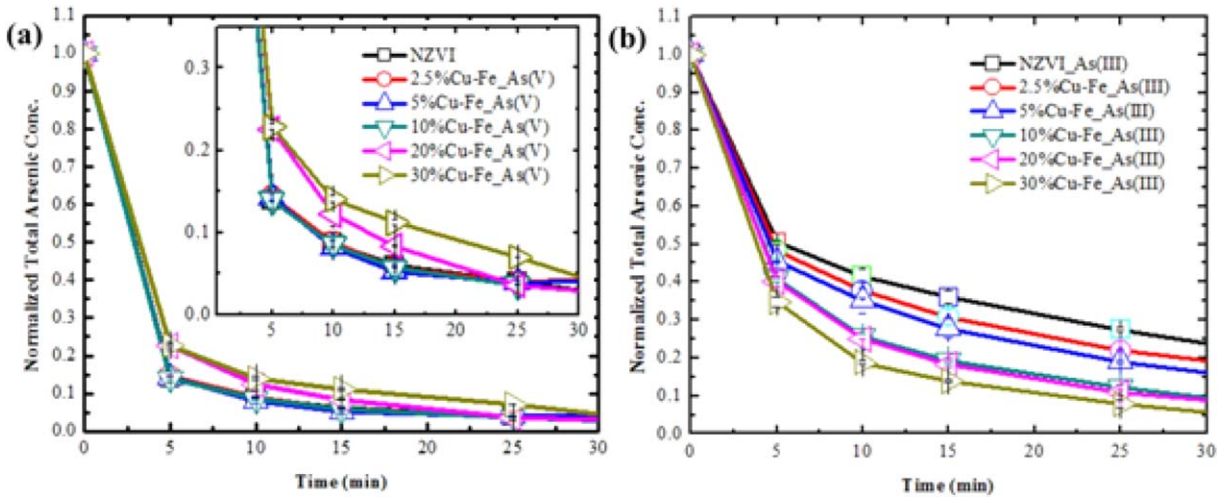

Figure 4. Effect of copper loading on bimetallic $(Cu\text{-}Fe)_{IM}$ in the presence of gas bubbling: (a) arsenate removal and (b) arsenite removal. [Color figure can be viewed at **wileyonlinelibrary.com**]

surface functional groups of NZVI. Regarding to the elemental analysis by EDX profiles, O, Fe, and Cu were found as major components with uniform dispersion on the surface of NZVI. With different synthesis techniques, the component of copper in the sample under IM method (8.49 wt %) was found higher than that by IS technique (7.55 wt %). Both techniques provided amount of Cu close to the nominal amount in preparation. Besides, it was found that Cu was deposited on surface of NZVI as a core-shell structure for IM synthesis method, while Cu was deposited inside NZVI as an alloyed structure for IS synthesis method.

TEM images with particle size distribution for each sample were shown in Figure 3. The average sizes of the iron nanoparticles were around 52, 46, and 32 nm for NZVI, $(Cu—Fe)_{IS}$, and $(Cu—Fe)_{IM}$, respectively. The morphology of nanoparticles exhibited two distinct layers; one represented NZVI itself as a core while an outer shell was covered with oxide species [17]. These two layers of materials might be due to the reaction between Fe, H_2O, and O_2, which could induce in the process of bimetallic synthesis, as described by Nakseedee *et al.* [15]. TEM image of $(Cu—Fe)_{IM}$ (Figure 3c) exhibits ultrafine nanoparticles uniformly dispersed on NZVI substrates, indicating the successful deposition of metallic Cu nanoscale on the surface of NZVI. Considering $(Cu—Fe)_{IS}$, copper might not distribute well on the surface. It would be due to an intraparticle mass diffusion effect during the scarification of Fe.

Table 1 presents specific areas of NZVI and 10% Cu—Fe in both synthesis methods. It was found that surface area was in the range of 22–30 $m^2\ g^{-1}$. An addition of the second material (Cu) with IM method into NZVI provided better surface area. However, the synthesis by IS method decreases surface area of Cu—Fe material.

As Removal Capability

Effect of Copper Loading

To investigate the enhancement of As removal by bimetallic Cu—Fe nanoscale, the effect of Cu loading was firstly investigated for 30 min of reaction. The IM method was chosen regarding on a higher removal performance and a simply preparation. Metal loadings of 2.5–30.0% w/w were prepared in series. As indicated in Figure 4, the As(III) and As(V) concentration profiles with different Cu loadings were dramatic decreased accompanied with the reaction time. The higher loading of Cu, the higher As(III) removal efficiency was.

Table 2. Pseudo-first order apparent rate constants of As removal.

	Rate constant (k, min^{-1})	
	As(III)	**As(V)**
$(Cu—Fe)_{IS}$	0.0357	0.0691
$(Cu—Fe)_{IM}$	0.0464	0.1489
NZVI	0.0222	0.1239

However, only a slight difference between among profiles of Cu loadings between 10, 20, and 30% were observed. An excess in Cu loading might promote an agglomeration of Cu particles, as indicated by TEM image, resulting in negative effect on the reactivity of $(Cu—Fe)_{IM}$. Thus, to further verify the appropriate synthesis method for Cu—Fe samples, the $10\%(Cu—Fe)_{IM}$ was preferred to conduct in the next step. To compare the performance of Cu—Fe with different synthesis methods, the kinetic analysis was carried out. The kinetic was presumed to be pseudo-first order reaction, and the results of analysis are tabulated in Table 2. Considering As(III) removal, it was found that the apparent rate constants [$k_{app} = 0.0464$ and 0.03757 min^{-1} for $(Cu—Fe)_{IM}$ and $(Cu—Fe)_{IS}$, respectively] were 2.1 and 1.6 times higher, respectively, than that of pristine NZVI ($k_{app} = 0.0222$ min^{-1}).

Effect of Synthesis Method

A comparison of As removal was further considered under IS and IM techniques. Figure 5 shows profiles of normalized total As concentrations along reaction time. Considering Cu loading of 10% as an example, it was found that the disappearance of As(III) over $(Cu—Fe)_{IS}$ and $(Cu—Fe)_{IM}$ were about 60 and 80% within 25 min of the reaction time, respectively. However, As(V) disappeared under $(Cu—Fe)_{IS}$ and $(Cu—Fe)_{IM}$ faster compared with As(III), as observed by 73 and 90% by 10 min of the reaction time, respectively. This was due to the difference in electrostatic attraction of two As species. The evidence showed in Figure 5c, the solution pHs during reaction were 4–6, which this range of pH, the dominant form of As(V) is $H_2AsO_4^-$ while As(III) is H_3AsO_3 [18]. As a previous study, the pH_{pzc} for NZVI synthesized was 7.8 [19]. As(V) presents charges oppositely for Cu—Fe particles while As(III) acts as neutral charge at the observed pH

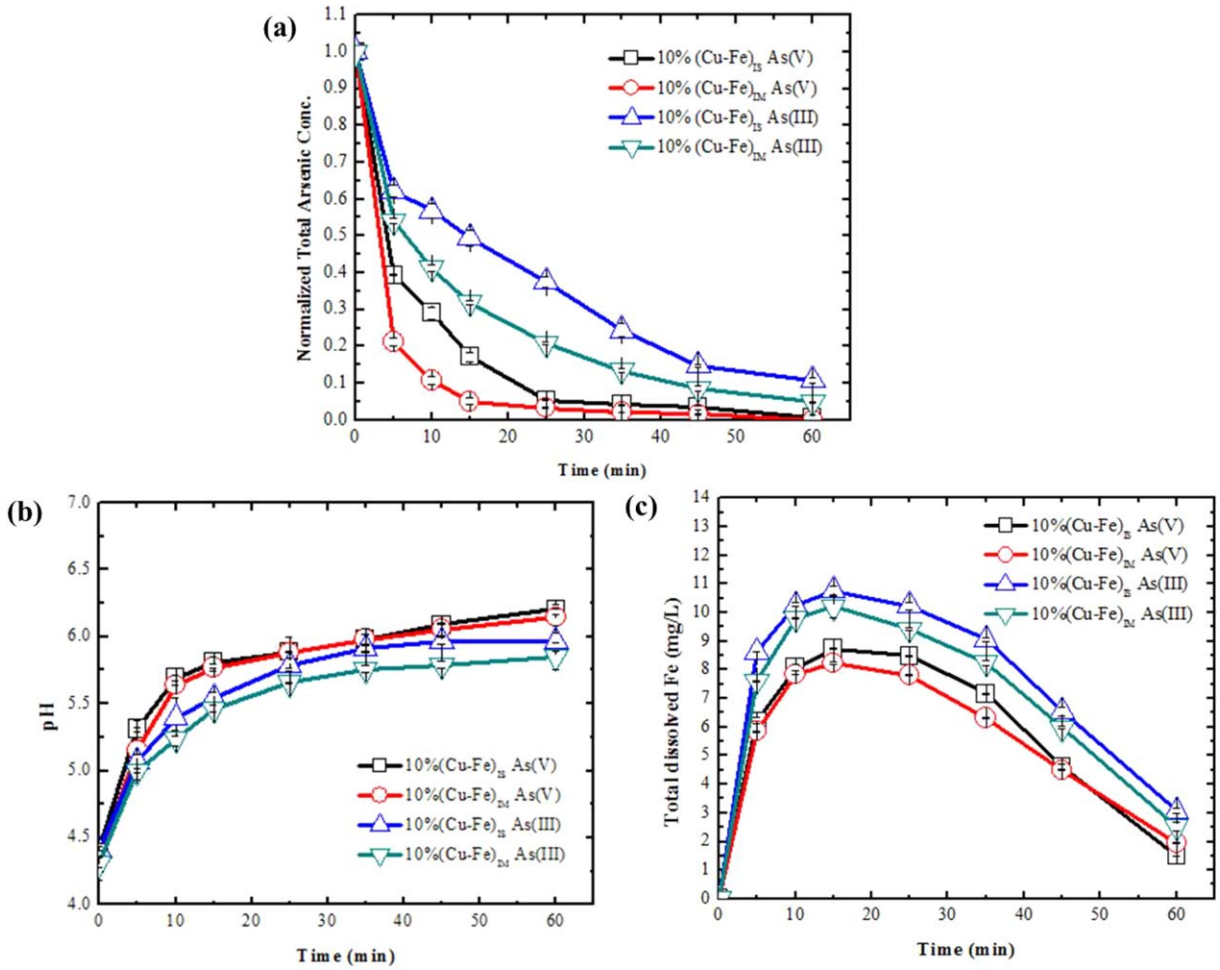

Figure 5. Profiles of (a) As(III) and As(V) removal under different synthesis methods (*in-situ* and impregnation reactions), (b) pH, and (c) total dissolved iron. [Color figure can be viewed at **wileyonlinelibrary.com**]

condition. An important note was that the removals of As in both species under $(Cu—Fe)_{IM}$ were much faster comparing with those under both pristine NZVI and $(Cu—Fe)_{IS}$.

During the reaction, pH and total dissolved iron have been monitored, as presented in Figures 5b and 5c. The pH condition of the solution was increased during the reaction, implying that an oxidation of zero valence iron took place, consequently releasing hydroxyl ions to the solution [20]. However, the pH profiles of the solution under loading Cu were not significantly different from each other. Considering on total dissolved iron in the solution, it refers to the amount of iron forms presented, including of Fe^{2+} and Fe^{3+} ions. In the initial state, the dissolved iron profiles increased due to the reaction between Fe^0 and dissolved oxygen. After 15 min of reaction, those oxidized forms of to Fe^{2+} and Fe^{3+} ions will further precipitate to iron (hydr)oxides, described in Eqs. (2–6) [19,21]. It caused the decrease of total dissolved Fe in the solution. Some of iron (hydr)oxides could combine with As(III) and As(V) through adsorption and coprecipitation [22,23].

$$Fe^{2+} + 2OH^- \rightarrow Fe(OH)_{2\downarrow} \quad (2)$$

$$Fe^{3+} + 3H_2O \rightarrow Fe(OH)_{3\downarrow} + 3H^+ \quad (3)$$

$$6Fe(OH)_{2\downarrow} + O_2 \rightarrow 2Fe_3O_{4\downarrow} + 6H_2O \quad (4)$$

$$Fe(OH)_{2\downarrow} + OH^- \rightarrow FeOOH_{\downarrow} + H_2O + e^- \quad (5)$$

$$2FeOOH_{\downarrow} + Fe^{2+} \rightarrow Fe_3O_{4\downarrow} + 2H^+ \quad (6)$$

Since the material consisted of not only Fe but also Cu, the standard redox potentials should be taken into account. The reduction potentials of Cu^{2+} and Fe^{2+} are 0.34 and −0.44 V, respectively. Copper ion therefore was likely to accept electrons, which were donated from NZVI. Consequently, NZVI was oxidized and became $Fe^{2+}$and further Fe^{3+} [24,25]. In addition, the profile of total dissolved iron using $(Cu—Fe)_{IM}$ is lower than that using$(Cu—Fe)_{IS}$ in both profiles of As(III) and As(V) removal, as seen in Figure 5c. The lower amount of dissolved iron could refer to the higher reactivity of formation toward iron (hydr)oxides and As—Fe complexes eventually [26].

To understand clearly and use to support the possible removal mechanism, active species of Cu—Fe samples should be investigated in detail. XANES technique was applied in this case for both fresh and spent materials using in the adsorption. The Fe XANES spectra and the detailed structure of the pre-edge peak for standard materials and Cu—Fe samples are illustrated in Figures 6a and 6b. It appears that each Cu—Fe sample is visually similar shoulder feature at 7114 eV; however, their centroids of white line peak are different suggested that there are various Fe oxides phases. Phases excluded from LCF of NZVI sample were Fe, Fe_3O_4, and

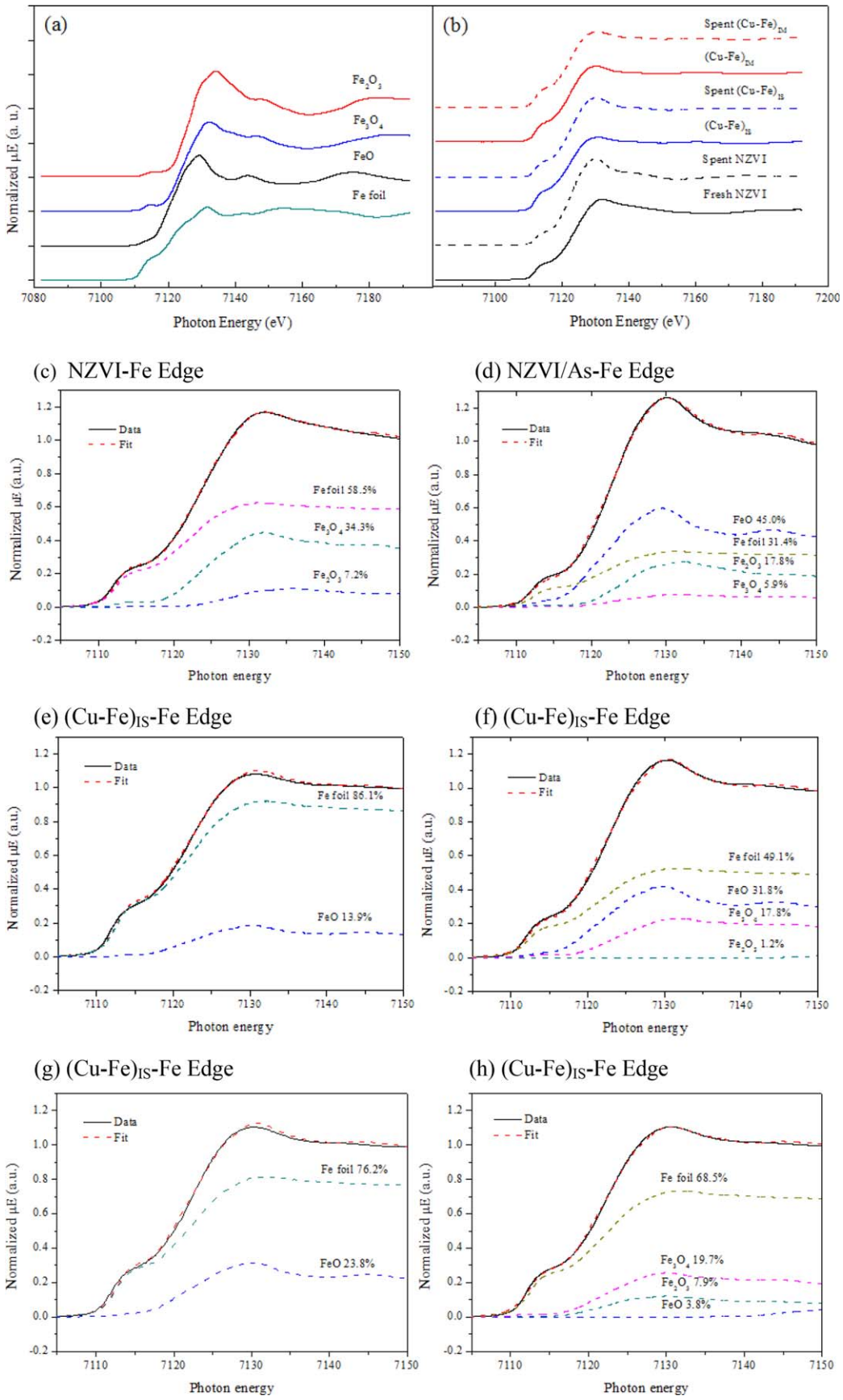

Figure 6. Normalized Fe K-edge XANES spectra of (a) the standards and (b) Cu-Fe samples accompanied with (g,h) the LCF of all samples. [Color figure can be viewed at **wileyonlinelibrary.com**]

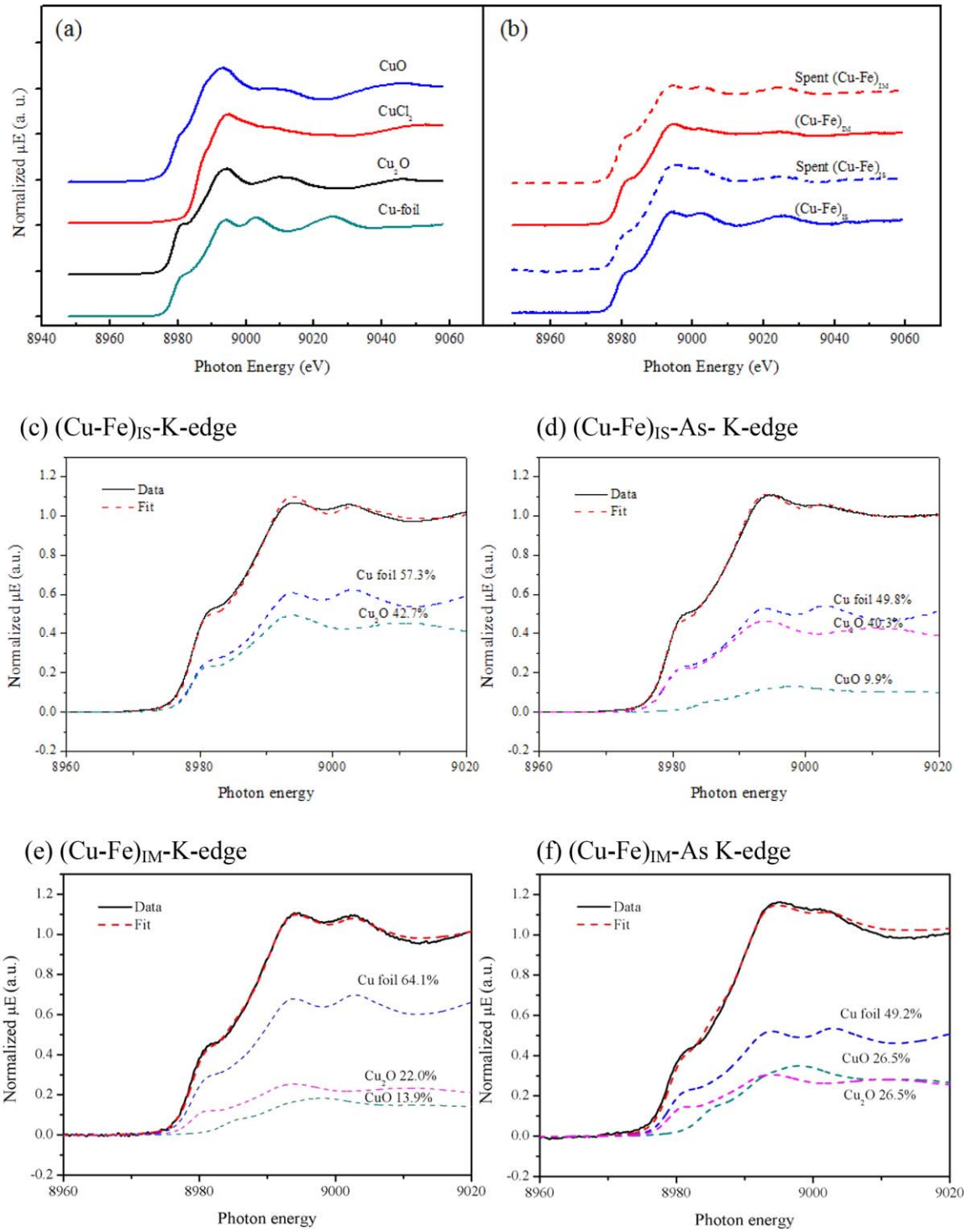

Figure 7. Normalized Cu K-edge XANES spectra of (a) the standards and (b) Cu-Fe samples accompanied with (c–f) the LCF of all samples. [Color figure can be viewed at **wileyonlinelibrary.com**]

Fe_2O_3while those of Cu—Fe samples were Fe and FeO Since the present phases of each spent samples (Figures 6g and 6h), four of which are readily identified as metallic Fe, FeO, Fe_2O_3, and Fe_3O_4. The decreases of observed metallic Fe concentration in reacted materials (as shown in Figures 6c–6h) are likely due to the formation of an iron mixed oxide phase. XANES spectra indicated that the apparent valence states of Fe of reacted Cu—Fe showed the decreasing of Fe content and the increasing of oxidized Fe form as seen in Figures 6e–6h. This confirms an ability of Cu to accelerate Fe oxidation.

Figure 7 shows XANES spectra of Cu K-edge. The spectra of the Cu—Fe samples are practically identical and very closely resemble the XANES spectra reported by Cu foil. Under the LCF analysis (Figures 7c–7f), it revealed that $(Cu—Fe)_{IS}$ possessed only Cu_2O phase while $(Cu—Fe)_{IM}$ contained a mixed phase of Cu_2O and CuO. After the adsorption process, metallic Cu was oxidized to Cu^{2+} as CuO form in spent material.

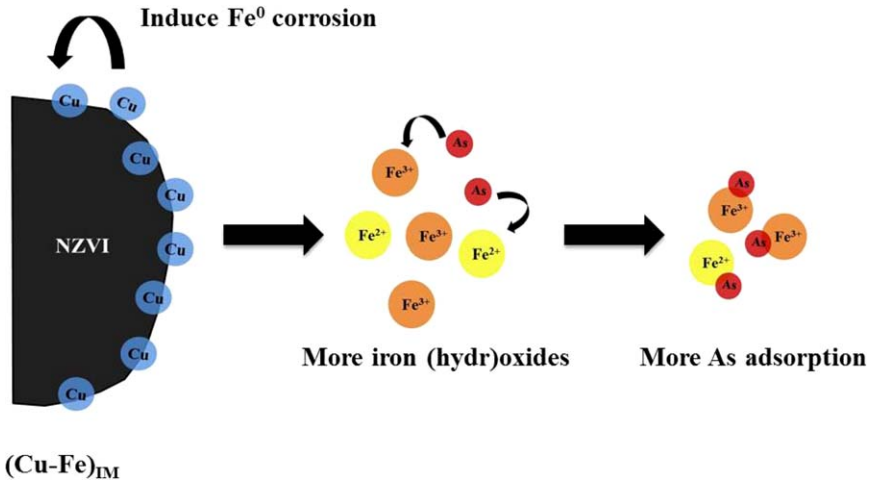

Figure 8. Proposed mechanism of As removal by using $(Cu\text{-}Fe)_{IM}$. [Color figure can be viewed at **wileyonlinelibrary.com**]

As known, the Standard Redox Potentials of Cu and Fe (shown in Eqs. (7) and (8)), the standard potential for copper is 0.34 volts, which is higher than that of iron (–0.44 volts). Consequently, copper probably accelerated the oxidation of Fe and form iron (hydr)oxides.

$$Cu^{2+} + 2e^- \rightarrow Cu_{(s)} \qquad E = 0.34\,V \tag{7}$$

$$Fe^{2+} + 2e^- \rightarrow Fe_{(s)} \qquad E = -0.44\,V \tag{8}$$

A mechanism of As removal by $(Cu—Fe)_{IM}$ could be postulated. The phenomena include precipitation and coprecipitation phenomena. The removal process is started with Cu^{2+} acting as an electron transfer to accept electron from Fe^0, resulting in Fe^{2+} and iron (hydr)oxides (Fe_xO_y) formation. The reaction proceeds continuously to cover all part of copper particles [27]. At this point, As is removed readily by a coprecipitation with Fe_xO_y, as shown in Figure 8.

CONCLUSION

Two different techniques, IS and IM, in synthesis of bimetallic Cu—Fe were employed in this study, comparing with bare NZVI and tested in As removal. Both $(Cu—Fe)_{IS}$ and $(Cu—Fe)_{IM}$ were used for As removal in the presence of CO_2 bubbling followed with air bubbling. The rate constant of As removal using $(Cu—Fe)_{IM}$ and $(Cu—Fe)_{IS}$ was around 3.77 and 4.66 times higher than other researches using aluminum and mild steel, respectively. As was significantly removed by $(Cu—Fe)_{IM}$ in both spiked DI and spiked groundwater conditions. Loading of 10% of Cu was found as an optimum loading. An impregnation technique provided Cu—Fe material in nanoparticles and higher Cu content on the surface. This enhanced iron corrosion rate and coprecipitation with As in the solution. The results from XANES spectra indicated that Fe could be more oxidized in the presence of Cu.

ACKNOWLEDGMENTS

This research was supported by Synchrotron Light Research Institute (Public Organization), Thailand.

LITERATURE CITED

1. Li, Z., Deng, S., Yu, G., Huang, J., & Lim, V.C. (2010). As(V) and As(III) removal from water by a Ce–Ti oxide adsorbent: Behavior and mechanism, Chemical Engineering Journal, 161, 106–113.
2. Kumar, M., Rahman, M.M., Ramanathan, A.L., & Naidu, R. (2016). Arsenic and other elements in drinking water and dietary components from the middle Gangetic plain of Bihar, India: Health risk index, Science of the Total Environment, 539, 125–134.
3. E.P.A. (2001). US, National Primary Drinking Water Regulations.
4. Korte, N.E., & Fernando, Q. (1991). A review of arsenic (III) in groundwater, Critical Reviews in Environmental Science and Technology, 21, 1–39.
5. Bang, S., Johnson, M.D., Korfiatis, G.P., & Meng, X. (2005). Chemical reactions between arsenic and zero-valent iron in water, Water Research, 39, 763–770.
6. Pillewan, P., Mukherjee, S., Meher, A.K., Rayalu, S., & Bansiwal, A. (2014). Removal of arsenic (III) and arsenic (V) using copper exchange zeolite-A, Environmental Progress & Sustainable Energy, 33, 1274–1282.
7. Tanboonchuy, V., Hsu, J.-C., Grisdanurak, N., & Liao, C.-H. (2011). Impact of selected solution factors on arsenate and arsenite removal by nanoiron particles, Environmental Science Pollution Research, 18, 857–864.
8. Watanabe, H., Mizuno, Y., Endo, T., Wang, X., Fuji, M., & Takahashi, M. (2009). Effect of initial pH on formation of hollow calcium carbonate particles by continuous CO_2 gas bubbling into $CaCl_2$ aqueous solution, Advanced Powder Technology, 20, 89–93.
9. Tanboonchuy, V., Grisdanurak, N., & Liao, C.-H. (2012). Background species effect on aqueous arsenic removal by nano zero-valent iron using fractional factorial design, Journal of Hazardous Materials, 205-206, 40–46.
10. Zhang, S., Niu, H., Cai, Y., Zhao, X., & Shi, Y. (2010). Arsenite and arsenate adsorption on coprecipitated bimetal oxide magnetic nanomaterials: $MnFe_2O_4$ and $CoFe_2O_4$, Chemical Engineering Journal, 158, 599–607.
11. Jiao, C., Cheng, Y., Fan, W., & Li, J. (2015). Synthesis of agar-stabilized nanoscale zero-valent iron particles and removal study of hexavalent chromium, International Journal of Environmental Science and Technology, 12, 1603–1612.
12. Cao, J., Xu, R., Tang, H., Tang, S., & Cao, M. (2011). Synthesis of monodispersed CMC-stabilized Fe–Cu bimetal nanoparticles for in situ reductive dechlorination of 1, 2, 4-trichlorobenzene, Science of the Total Environment, 409, 2336–2341.
13. Bransfield, S.J., Cwiertny, D.M., Roberts, A.L., & Fairbrother, D.H. (2006). Influence of copper loading and surface coverage on the reactivity of granular iron toward

1,1,1-trichloroethane, Environmental Science & Technology, 40, 1485–1490.
14. Xue, X., Lv, X., Jiang, G., Baig, S.A., & Xu, X. (2016). Influence of Environmental Factors on Hexavalent Chromium Removal From Aqueous Solutions by Nano-Adsorbent Composites, Clean: Soil Air Water, 44, 162–168.
15. Nakseedee, P., Tanboonchuy, V., Pimpha, N., Khemthong, P., Liao, C.-H., & Grisdanurak, N. (2015). Arsenic removal by nanoiron coupled with gas bubbling system, Journal of Taiwan Institute of Chemical Engineering, 47, 182–189.
16. Khemthong, P., Photai, P., & Grisdanurak, N. (2013). Structural properties of CuO/TiO_2 nanorod in relation to their catalytic activity for simultaneous hydrogen production under solar light, Internatinal, Journal of Hydrogen Energy, 38, 15992–16001.
17. Yan, W., Herzing, A., Kiely, C., & Zhang, W. (2010). Nanoscale zero-valent iron (nZVI): aspects of the core-shell structure and reactions with inorganic species in water, Journal of Contaminant Hydrology, 118, 96–104.
18. Raven, K.P., Jain, A., & Loeppert, R.H. (1998). Arsenite and arsenate adsorption on ferrihydrite: kinetics, equilibrium, and adsorption envelopes, Environmental Science & Technology, 32, 344–349.
19. Tanboonchuy, V., Hsu, J.-C., Grisdanurak, N., & Liao, C.-H. (2011). Gas-bubbled nano zero-valent iron process for high concentration arsenate removal, Journal of Hazardous Materials, 186, 2123–2128.
20. Choi, N.-C., Kim, S.-B., Kim, S.-O., Lee, J.-W., & Park, J.-B. (2012). Removal of arsenate and arsenite from aqueous solution by waste cast iron, Journal of Environmental Sciences, 24, 589–595.
21. Lackovic, J.A., Nikolaidis, N.P., & Dobbs, G.M. (2000). Inorganic arsenic removal by zero-valent iron, Environmental Engineering Science, 17, 29–39.
22. Tyrovola, K., Peroulaki, E., & Nikolaidis, N.P. (2007). Modeling of arsenic immobilization by zero valent iron, European Journal of Soil Biology, 43, 356–367.
23. Banerjee, K., Helwick, R.P., & Gupta, S. (1999). A treatment process for removal of mixed inorganic and organic arsenic species from groundwater, Environmental Progress & Sustainable Energy, 18, 280–284.
24. Furukawa, Y., Kim, J-w., Watkins, J., & Wilkin, R.T. (2002). Formation of ferrihydrite and associated iron corrosion products in permeable reactive barriers of zero-valent iron, Environmental Science & Technology, 36, 5469–5475.
25. Triszcz, J.M., Porta, A., & Einschlag, F.S.G. (2009). Effect of operating conditions on iron corrosion rates in zero-valent iron systems for arsenic removal, Chemical Engineering Journal, 150, 431–439.
26. Huang, Y.H., & Zhang, T.C. (2005). Effects of dissolved oxygen on formation of corrosion products and concomitant oxygen and nitrate reduction in zerovalent iron systems with or without aqueous Fe^{2+}, Water Research, 39, 1751–1760.
27. Hu, C.-Y., Lo, S.-L., Liou, Y.-H., Hsu, Y.-W., Shih, K., & Lin, C.-J. (2010). Hexavalent chromium removal from near natural water by copper–iron bimetallic particles, Water Research, 44, 3101–3108.